

Predicting patterns of long-term adaptation and extinction with population genetics

J Bertram¹, K Gomez², and J Mase¹

¹*Department of Ecology and Evolutionary Biology, University of Arizona,
Tucson, AZ 85721*

²*Program in Applied Mathematics, University of Arizona, Tucson, AZ 85721*

November 8, 2021

To whom correspondence should be addressed. E-mail: jbertram@email.arizona.edu
and mase@email.arizona.edu.

Running title: Population genetics of gradual extinction

Keywords: Genetic load, Red Queen, Cost of selection, Eco-evolutionary
dynamics, Reverse-time Markov chain

Abstract

Population genetics struggles to model extinction; standard models track the relative rather than absolute fitness of genotypes, while the exceptions describe only the short-term transition from imminent doom to evolutionary rescue. But extinction can result from failure to adapt not only to catastrophes, but also to a backlog of environmental challenges. We model long-term evolution to long series of small challenges, where fitter populations reach higher population sizes. The population’s long-term fitness dynamic is well approximated by a simple stochastic Markov chain model. Long-term persistence occurs when the rate of adaptation exceeds the rate of environmental deterioration for some genotypes. Long-term persistence times are consistent with typical fossil species persistence times of several million years. Immediately preceding extinction, fitness declines rapidly, appearing as though a catastrophe disrupted a stably established population, even though gradual evolutionary processes are responsible. New populations go through an establishment phase where, despite being demographically viable, their extinction risk is elevated. Should the population survive long enough, extinction risk later becomes constant over time.

Extinction has historically been viewed in two different ways (Maynard Smith, 1989; Raup, 1994; MacLeod, 2014): the “catastrophic” view, which revolves around sudden, severe disturbances; and the “gradualist” view, which emphasizes long-term evolutionary processes such as failure to adapt to slowly deteriorating circumstances. While catastrophes are bound to occur eventually, and present an obvious danger when they do, the threat posed by cumulative changes in the environment (both biotic and abiotic) is no less serious. Although the deleterious effects of these changes can be partly mitigated by physiological or behavioral adaptation, if they are not offset by evolutionary adaptation, and begin to accumulate, extinction is inevitable (Bürger and Lynch, 1995).

The catastrophic and gradualist views are not mutually exclusive. A population’s vulnerability to additional disturbances depends on its current burden of adaptive failures or “lag load” (a measure of the fitness distance between a genotype and a perfectly adapted genotype; Maynard Smith 1976), which may have accumulated gradually. Thus, even in cases where extinction is proximately caused by major disturbances, long-term evolution may have exerted a strong influence on the extinction process. Yet relatively little is

known about gradual extinction processes (Bürger and Lynch, 1995), especially when compared to the celebrity of catastrophes in paleontology (Raup, 1994; MacLeod, 2014) and conservation biology (Barnosky et al., 2011).

We identify three main existing classes of gradual extinction model (Table 1). First, applying classical population genetics theory, Haldane (1957) gave the first quantitative theoretical predictions of the time scales and risks associated with long-term evolution by considering the number of deaths attributable to selection during a single selective substitution — the “cost” of selection. Measured as a proportion of population size (N), this gives an estimate of the fitness reduction during substitution (“substitutional load”), or the number of generations needed for substitution. While not directly predicting extinction risk, substitutional load arguments attempt to identify limits to the rate of adaptation.

Second, probably the most well-known model of gradual extinction is Bürger and Lynch’s quantitative genetics model of stabilizing selection on a single trait, where environmental change is represented by change in the optimal trait value (Bürger and Lynch, 1995; Gomulkiewicz and Houle, 2009). Population size is finite, so extinction will occur eventually because of demographic stochasticity, regardless of environmental change. However, extinction occurs much more rapidly when the environmental change rate exceeds a critical value at which the mean phenotype lags so far behind its optimum that demographic decline ensues (mean absolute fitness falls below one). Bürger and Lynch (1995) calculated this critical environmental change rate as well as times to extinction, although individual-based simulations were needed for most of their predictions.

Third, the adaptive dynamics approach has been used to explore the consequences of feedbacks between evolution and ecology in communities of evolving species (Dieckmann and Ferrière, 2004). Adaptive dynamics describes evolution as a sequence of “trait substitutions”, in which one species at a time in a community is invaded by an adaptive mutant (each species has a single trait value), moving the community from one ecological equilibrium to a neighbouring one. The consequences for extinction can be dramatic; species may drive themselves extinct via trait substitution sequences (“evolutionary suicide”), even in the absence of abiotic environmental change or evolutionary change in other species (Ferrière and Legendre, 2012). The published extinction predictions of adaptive dynamics have so far been primarily descriptive (Ferrière and Legendre, 2012).

Here we present a new model of long-term adaptation and extinction

that builds upon and extends previous work. Like Bürger and Lynch (1995), we assume that extinction is driven by gradual environmental deterioration. Extinction can be avoided by evolutionary adaptation, which depends on genetic and demographic factors. However, our model is based on population genetics rather than quantitative genetics, and is not restricted to quantitative traits. As a result, individual mutations can have large or intermediate effects in our model rather than only modifying quantitative trait loci of small effect; the former are known to be important drivers of adaptation (Orr, 2005).

Similar to adaptive dynamics, we recognize the importance of feedbacks between long-term evolutionary changes and the short-term demographic response of the population. We restrict our attention to changes in the focal population size N without modeling the complex response of entire ecological communities. Poorly adapted populations will generally have fewer individuals, which reduces adaptive mutant production and increases the chance of further fitness decline, reminiscent of a “mutational meltdown” (Lynch et al., 1993). However, in low fitness populations, more beneficial mutations will be available (there are more problems to be addressed). Each beneficial mutation will also have a greater effect compared to when fitness is high (diminishing returns epistasis; Wiser et al. 2013).

Our model is based on Desai and Fisher’s (2007) asexual traveling wave model, under which the steady state adaptation rate is determined by a balance between selection and beneficial mutations. In that model, as in most population genetic models, N is constant over time and evolution occurs along a relative fitness axis; thus extinction is impossible. To model extinction, we replace relative fitness with a simple model of density-dependent absolute fitness, so that N changes dynamically. The beneficial mutation rate is assumed to depend on absolute fitness. In addition, we introduce a Markov chain approximation for the population’s long-term evolution, which is considerably simpler than the full traveling wave model.

We use our model to explore a few basic questions about long-term evolution: (1) What are the conditions for long-term persistence, and are persistence times predicted from our micro-evolutionary model consistent with macro-evolutionary persistence times in nature? (2) What is the distribution of extinction times? (3) Should we expect to be able to distinguish gradual from catastrophic causes of extinction based on observations of a population’s behavior prior to extinction?

Approach	Genetics	Fitness-dependent population size	Fitness-dependent mutation rate	Extinction predictions
Quantitative genetics (Bürger & Lynch 1995)	Small effects at a large number of loci.	No	No	Critical rates, extinction times
Substitutional load (Haldane 1995)	Single locus substitution	No	No	Number of selective deaths required for substitution
Adaptive dynamics (Dieckmann & Ferrière 2004)	No explicit genetics	Yes	No	Evolutionary suicide (qualitative)
Traveling wave (relative fitness) (Desai & Fisher 2007)	Linkage disequilibrium	No	No	N/A
This paper	Linkage disequilibrium	Yes	Yes	Critical rates, extinction times

Table 1: Comparison of this paper with related models.

Model

Following Desai and Fisher (2007), the population is divided into discrete fitness classes differing by multiples of a constant fitness increment s (Fig. 1). Population size N is assumed to be large enough that the abundances of most fitness classes behave deterministically. Desai and Fisher (2007) is formulated in terms of relative fitness, and N is constant. We instead use a simple logistic model of absolute fitness,

$$\frac{1}{n_i} \frac{dn_i}{dt} = b \left(1 - \frac{N}{\kappa} \right) - (d + is). \quad (1)$$

Here n_i is the abundance of fitness class i (so that $N = \sum_i n_i$), b is the intrinsic birth rate, d is the mortality rate of perfectly adapted ($i = 0$) individuals, and is is the additional mortality associated with fitness class i . The indices i count the number of fitness classes from perfection, and can therefore be interpreted as a measure of lag load (Maynard Smith, 1976). κ is the maximum possible population size without deaths, representing territorial or resource limitations. Henceforth, the index i will be used to refer to any possible fitness class, which could be empty, while j will be used to

refer specifically to the most fit class that has abundance large enough that it behaves approximately deterministically according to Eq. (1) (Fig. 1).

κ is distinct from the maximum achievable abundance (the carrying capacity), where births balance deaths ($dN/dt = 0$). If all individuals are in the same fitness class j , the carrying capacity is $K_j = (b - d - js)\kappa/b$, which decreases with decreasing fitness. The population is not viable if deaths exceed births at low population density i.e. $d + is > b$ for all occupied fitness classes. This defines an extinction threshold $i_e \approx (b - d)/s$, given by the i where $d + is$ first exceeds b .

We only consider beneficial mutations, and all mutations have the same fitness effect s irrespective of genetic background. We assume that the beneficial mutation rate in fitness class i is Ui per birth, where U is a constant. This represents a “running out of mutations” effect, where there are more ways for genetic novelty to improve fitness in poorly-adapted genotypes (and no ways to improve a perfect genotype). We return to our running out of mutations assumption, specifically how it differs from diminishing returns epistasis, in the Discussion.

There is no sex, so mutations only matter in the leading deterministic class j , producing mutants appear in the stochastic “nose” $j - 1$. Mutations on poorer genetic backgrounds — away from the nose — are doomed to be outcompeted by nose mutants (multiple-mutations interference; Desai and Fisher 2007). Thus, the only relevant mutation rate in our model is that feeding the nose Uj .

Mutant lineages initially have low abundance (starting from a solitary mutant), and are therefore strongly affected by demographic stochasticity. Only some mutant lineages avoid going extinct in the initial stochastic phase and attain a large enough abundance that they grow deterministically according to Eq. (1) (a process called “establishment”). The probability of establishment at the nose, denoted p_{j-1} , is approximately $q_js/(d + js)$ for most mutations (Appendix A), where $q_j = \bar{i} - (j - 1)$ is the number of fitness classes that the nose is ahead of the mean (Fig. 1). However, p_{j-1} can be substantially smaller if environmental change occurs during the establishment process. The calculation of p_{j-1} in this case is discussed in Appendix A.

Once a mutant lineage established, it becomes the new most fit established class with dynamics governed by Eq. (1). The initial abundance for deterministic growth ν , which is applied at the time that the mutation occurs, is a random variable that represents the stochasticity in the time that the mutant lineage takes to establish. The cumulative density function for ν

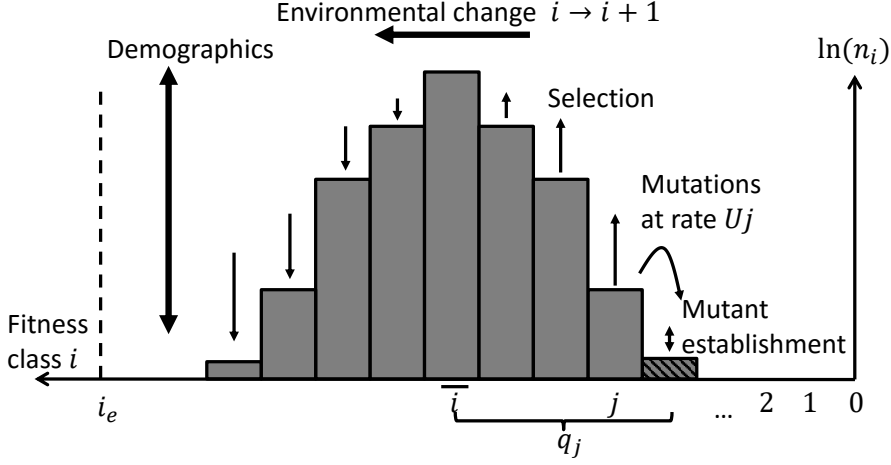


Fig. 1: Absolute fitness classes i representing fitness increments of size s , with abundances n_i . Environmental deterioration intermittently reduces population fitness by s . Fitness classes grow or decline relative to each other depending on whether their fitness is respectively greater or smaller than the mean fitness \bar{i} (small vertical arrows). Population size N changes dynamically with fitness (double-headed vertical arrow). At the nose of the distribution, mutant establishment is stochastic (hatched bar). The fittest established class is j , and mutants are $q_j = \bar{i} - (j - 1)$ fitness classes away from the mean (their fitness advantage is $q_j s$). The extinction threshold i_e is shown with a vertical dashed line.

is given by (Uecker and Hermisson, 2011, Eq. 40)

$$P(\nu \leq \nu_0) = 1 - e^{-\nu_0 p_{j-1}}, \quad (2)$$

so that the mean of ν is $1/p_{j-1}$ (also see Desai and Fisher, 2007, Eq. 16).

Note that there is a clean separation between the deterministic bulk obeying Eq. (1), with fittest class j , and the stochastic nose in fitness class $j - 1$, as shown in Fig. 1. This clean separation holds when establishing mutants make up a small fraction of the population ($Ns \gg 1$), and Uj is small enough that mutant lineages rarely produce double-mutants before establishment (birth rate $\times Uj \ll s$; Desai and Fisher 2007), as is the case here.

Environmental deterioration occurs in discrete events where the entire fitness distribution is shifted backwards by one fitness class ($i \rightarrow i + 1$ for all of the population's fitness classes). These events are assumed to follow

a Poisson process with mean time T between successive changes. Thus, in addition to being a measure of lag load, i can also be interpreted as the number of environmental challenges facing the individuals in fitness class i . In this interpretation, the linear dependence of the mutation rate Uj on j can be interpreted as saying that each environmental deterioration event opens up one new possible beneficial mutation that addresses the new environmental challenge.

Environmental challenges may be biotic or abiotic in our model; fitness differences simply represent differences in mortality without specifying causes. We could easily attribute fitness differences in Eq. (1) to births or a mixture of births and deaths instead, but this would not substantially alter our model’s behavior.

Results

The model described above is simulated numerically (implementation is summarized in Supplement A). In addition to these simulations, we show that the population’s long-term evolution can be approximated with a much simpler discrete-time Markov chain (MC).

Markov chain approximation

Our model has two distinct adaptive regimes: the “successional” regime, and the “multiple mutations” regime. We first describe our MC approximation in the “successional” regime, where fixation (the growth of a newly established mutant to a frequency of 1) is much faster than the typical time between mutant establishments. The population spends most of the time in equilibrium with all individuals in one fitness class j ($N \approx K_j$), waiting for adaptive mutant establishment or environmental change. Adaptive advances occur at a mean rate v_j equal to the equilibrium birth rate $K_j b(1 - K_j/\kappa)$ multiplied by the mutation rate Uj and establishment probability p_{j-1} ,

$$v_j = K_j b(1 - K_j/\kappa) Uj p_{j-1}. \quad (3)$$

Our MC approximation amounts to taking regular “snapshots” at intervals given by the characteristic fixation time (Appendix B). In the vast majority of snapshots, the population will be in equilibrium, and will jump between

fitness classes with per-snapshot probabilities proportional to $1/T$ for environmental change $j \rightarrow j + 1$, and v_j for adaptive mutant fixation $j \rightarrow j - 1$. These are the MC transition probabilities. The current MC state is j , with possible values $i = 0, \dots, i_e$ (Fig. 2a), and each MC iteration represents the fixation time. The extinction threshold i_e is an absorbing state because the corresponding $N = 0$ equilibrium is attained within a single iteration (the scenario where the extinction threshold has been crossed but the population manages to recover by producing higher-fitness individuals with $i < i_e$, called “evolutionary rescue”, is not possible in our MC approximation).

In the “multiple mutations” regime, fixation is slower than the rate at which mutants destined for establishment are produced, and there is standing fitness variation ($q_j > 0$). By invoking beneficial mutation-selection balance, the steady-state adaptation rate can be approximated analytically for a given mutation rate, population size and establishment probability (Desai and Fisher, 2007). The latter quantities depend on fitness, particularly the position of the most fit established class j . Thus, the corresponding steady state also depends on j , giving (Appendix C)

$$q_j \approx \frac{2 \ln(K_j s)}{\ln(s/Uj)}, \quad v_j \approx \frac{2 \ln(K_j s) - \ln(s/Uj)}{\ln^2(s/Uj)} s. \quad (4)$$

This is a straightforward generalization of Eqs. (40) and (41) in Desai and Fisher (2007), which assumed constant mutation rate, population size and establishment probability.

Unlike the successional regime MC approximation, adaptation cannot be treated as memoryless (independent of the population’s history) in the multiple mutations MC approximation. The mutant-generating class j grows over time, and thus so does the overall rate of mutant production at the nose. Consequently, mutant establishment is much less likely shortly after the previous establishment, while class n_j is still small. Moreover, previous growth at the nose is not “forgotten” when environmental changes occur. Thus, mutant establishments occur more regularly than memoryless events with mean rate v_j . Accordingly, we use two MC approximations to bound the actual behavior of the multiple mutations regime. In the first, we ignore memory so that v_j from Eq. (4) is the $j \rightarrow j - 1$ transition probability, analogous to the successional case (Fig. 2a). In the second, we assume that mutant establishment occurs periodically at given intervals (Fig. 2b). Each iteration of the periodic-adaptation MC represents the time required for mutant establishment $1/v_j$, and exactly one establishment happens every iteration. Note that

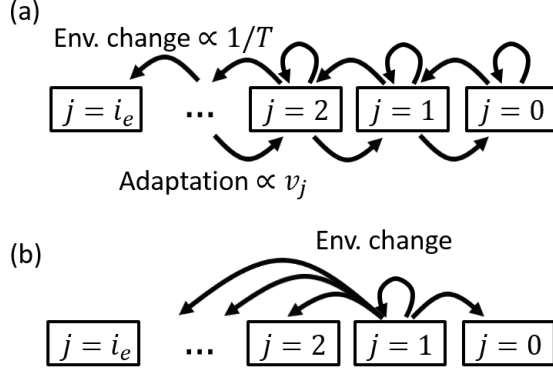


Fig. 2: In addition to simulations of the traveling wave model illustrated in Fig. 1, two Markov chain approximations are used to model long-term evolution. (a) Memoryless adaptation with $j \rightarrow j - 1$ transition probability proportional to v_j where j is the fittest established class, and v_j is given by Eq. (3) (successional regime) and Eq. (4) (multiple-mutations regime). (b) Periodic adaptation in the multiple mutations regime, where each iteration represents the establishment timescale $1/v_j$. Exactly one adaptation event occurs each iteration, but a variable number of environmental change events can occur.

the memoryless and periodic-adaptation MC chains differ only in whether or not *adaptation* is memoryless: in both cases, the transition probabilities are memoryless, as they must be in a Markov chain. The mathematical details of our MC approximation are given in Appendix B.

Extinction times

Long-term evolution is primarily controlled by the difference between the opposing rates of environmental change $1/T$ and adaptation v_j , where v_j tends to zero at perfection $j = 0$ (no beneficial mutations) and extinction $j = i_e$ ($N = 0$), and exhibits a peak between these extremes (Fig. 3a). Figure 3b shows the predicted pattern of time to extinction t_e versus T (time is measured in generations, implemented by setting $d = 1$). When environmental change is relatively rapid ($T < 150$), the population cannot keep up with environmental deterioration ($1/T > v_j$ for all j), and extinction occurs rapidly (thousands of generations). Modestly slowing environmental

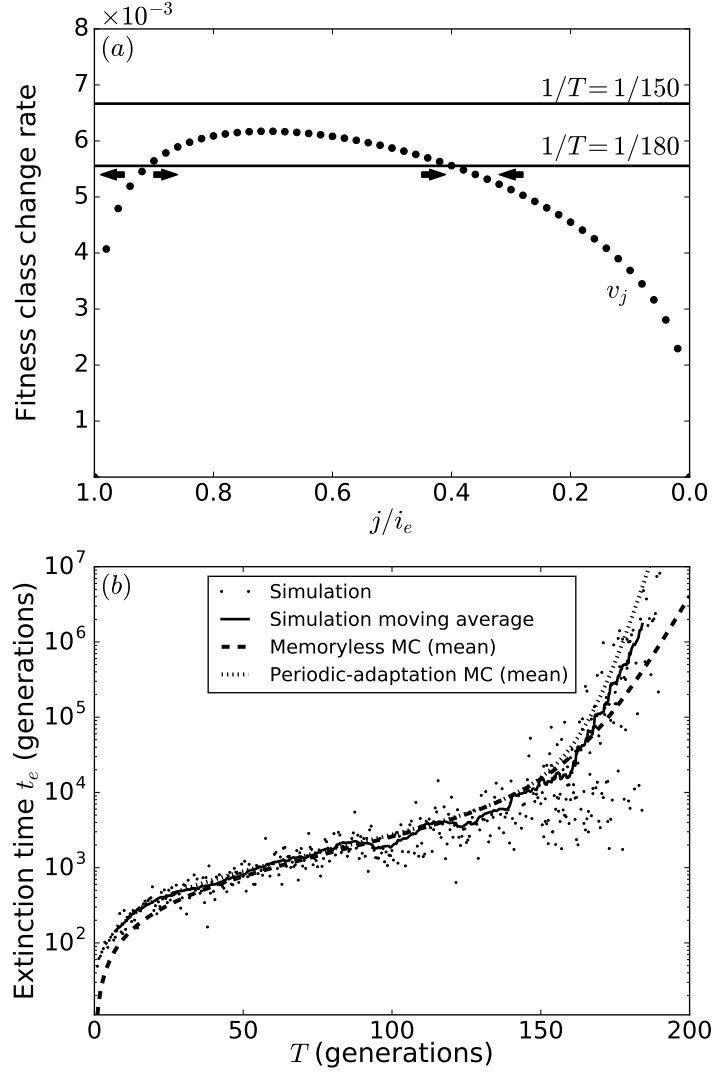


Fig. 3: Time to extinction t_e increases abruptly with increasing T . (a) As T increases, the population transitions from “always losing” to “sometimes winning”. Arrows show mean direction of fitness change near points where $1/T = v_j$; $j/i_e \approx 0.4$ is an “attractor”. (b) Comparison of simulated t_e and mean t_e predicted from MC approximation (Appendix B). Parameters: $b = 2, d = 1, U = 10^{-6}, s = 0.02, \kappa = 4 \times 10^6, j_{\text{initial}}/i_e = 0.4$ (multiple mutations regime).

change ($T = 180$) allows the population to beat the environment ($1/T < v_j$) over part of the fitness domain, dramatically increasing the mean and variance in t_e (compare Bürger and Lynch, 1995, Fig. 1b). This sudden transition to long-term persistence occurs at $T \approx 160$. Fig. 3 is in the multiple mutations regime; the successional regime gives essentially identical results, except with lower persistence times for given T (since, by definition, there are far fewer adaptive mutants establishing).

MC mean extinction times $\langle t_e \rangle$ (Appendix B) closely follow the full simulation results (Supplement A) in Fig. 3b. The periodic-adaptation MC performs better than the memoryless MC, confirming the importance of mutant establishment “memory” in the multiple mutations regime.

Fig. 4a shows the distribution of extinction times for a population with low initial fitness $j_{\text{initial}}/i_e = 0.8$ (compare Bürger and Lynch, 1995, Fig. 4). This could represent a newly establishing population at the start of peripatric speciation, for example. As expected, the distribution is sharply peaked near zero, reflecting a high risk of early extinction. The distribution also has a long tail (Fig. 4a inset), reflecting cases where the population manages to reach the stable “attractor” at $j/i_e \approx 0.4$ (Fig. 3a). Once the attractor is reached, long-term persistence is possible.

The tail in the distribution of t_e is exponential (Fig. 4a inset), indicating that extinction risk is effectively constant over time. The reason for this constant risk is that the population remains near the attractor for most of its existence. When extinction does occur, it is due to an abnormally rapid sequence of environmental changes and/or slow sequence of mutant establishments rather than a gradual erosion of fitness. The resulting decline in fitness is rapid compared to the mean persistence time. Fig. 5 shows the average decline in fitness immediately prior to extinction obtained by averaging over simulated trajectories in the full model as well as a backward-time variant of our MC approximation (Supplement B); moving from the attractor to the extinction threshold only takes around 1% of mean persistence time.

This explains why such a substantial discrepancy exists between the memoryless MC and simulations after the transition to persistence ($T > 160$), but not before it ($T \approx 100$): after the transition, large fluctuations in the number of adaptive establishments are much more likely when establishments are memoryless. Before the transition, there is no attractor, mean time to extinction is determined by the average decline in fitness due to the fact that $1/T < v_j$ (specifically, $\langle t_e \rangle = j_{\text{initial}}/(1/T - v_j)$), and fluctuations are only of secondary importance.

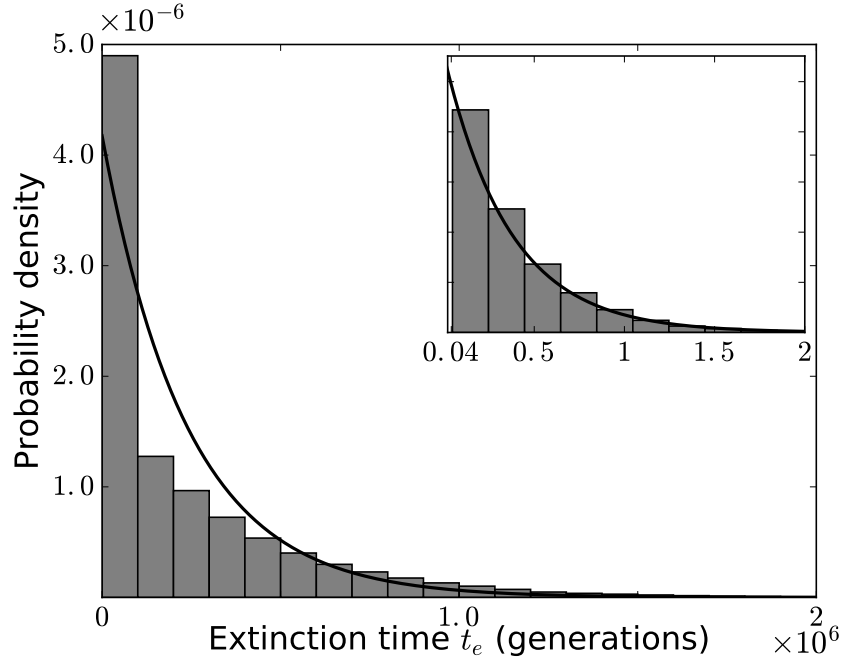


Fig. 4: The distribution of extinction times for fixed T is not exponential, but has an exponential tail. Main figure: t_e from memoryless MC simulations (histogram; same parameters as Fig. 3 except $j_{\text{initial}}/j_e = 0.8$) compared with the corresponding (same mean) exponential distribution (curve). Inset: same simulations omitting the initial spike of rapid extinction $t_e < 4 \times 10^5$ (histogram). Curve shows exponential distribution with mean given by MC mean t_e (using Eq. (B2)) assuming $j_{\text{initial}}/j_e = 0.4$ (the attractor in Fig. 3).

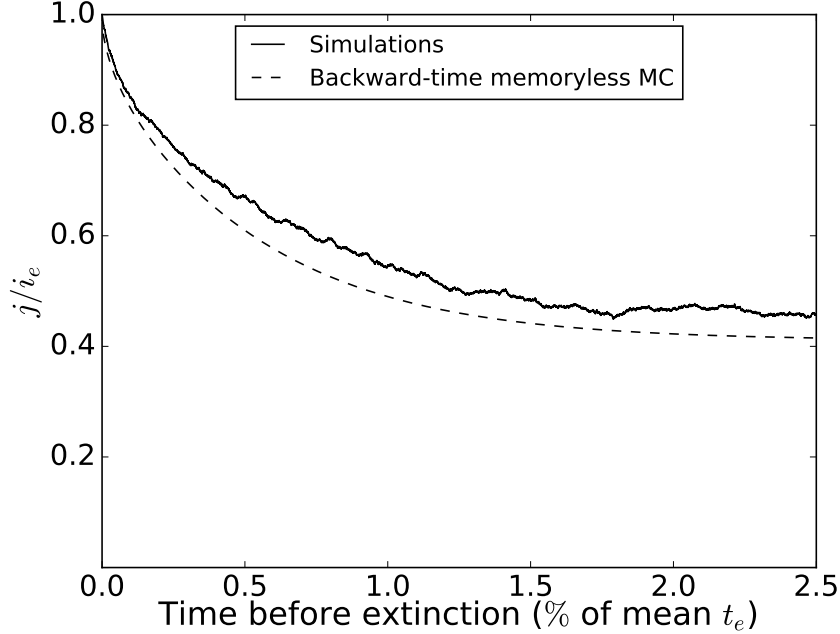


Fig. 5: For persistent populations, fitness declines rapidly at the time of extinction compared to mean t_e . Shown is the expectation of j for the backward-time trajectory immediately preceding extinction, using both backward-time memoryless MC (Supplement B) and averaging over simulated trajectories in the full model. Mean persistence time is $\approx 2 \times 10^6$ generations. Same parameters as Fig. 3 with $T = 180$.

Discussion

It is difficult to directly compare our predictions with fossil data because we have only considered a single population adapting to local environmental changes. Fossil extinction times also reflect larger scale processes in which environmental heterogeneity, range shifts and migration are potentially important. Nevertheless, population-level processes should have a strong influence at larger spatial and temporal scales, particularly for species with relatively small ranges.

For concreteness, consider the example of mollusc species, which feature prominently in the fossil record, and can have tiny geographic ranges (Stanley, 1986). A representative generation time for fossil mollusc species is on

the order of 10 years (Powell et al., 2011). With this generation time, our extinction time predictions (Fig. 3) are easily large enough to be consistent with typical fossil species persistence times of several million years (Raup, 1994). The shortest interval between environmental changes consistent with long-term persistence is $T \approx 160$ generations, or approximately a 2×10^3 years between 2% increases in mortality rate (since $d = 1$ and $s = 0.02$). By comparison, the major glacial cycles in the last 1 million years occurred at intervals of roughly 10^5 years (Augustin et al., 2004). Thus, in the absence of adaptation, the mortality rate would roughly double over the course of each major glaciation cycle. This rate of environmental change is certainly gradual compared to catastrophes such as the aftermath of bolide impacts, but is still rapid enough to present a significant threat to long-term persistence. Accordingly, the long-term persistence of our population is not a trivial consequence of a negligible environmental threat. Our population size, which is order 10^6 individuals (except when close to extinction), is considerably smaller than is typical for extant molluscs (Stanley, 1986), and can be viewed as a conservative lower bound (in any case, v_j only increases logarithmically with N in Eq. (4)). These results provide a rare bridge between micro-evolutionary population genetic models and macro-evolutionary phenomena

The fossil record contains many instances of abundant, widely-distributed species that have suddenly disappeared. This is commonly cited in support of a catastrophic view of extinction (Raup, 1994). In contrast, Darwin seems to have regarded sudden disappearance as a fossilization artifact, holding that species typically disappear gradually “first from one spot, then from another, and finally from the world” (Darwin, 1859, pp. 317), driven by inter-specific competition (Raup, 1994). Thus, there is no need to “invoke cataclysms to desolate the world” (Darwin, 1859, pp. 73). These viewpoints share the questionable assumption that sudden disappearance — assuming it is not an artifact — indicates a severe, sudden driver of extinction. This clearly need not be true in light of the suddenness of extinction in our gradualist model (Fig. 5), which would appear as a long period of relatively stable abundance followed by sudden disappearance. Sudden disappearance is driven entirely by gradual evolutionary processes, not the one or few extreme environmental changes that characterize catastrophes. In a sense it is still a “catastrophe” — an abnormally large fitness fluctuation — but this fluctuation reflects poor adaptive performance just as much as environmental pressure. Thus, sudden disappearance alone does little to distinguish between catastrophic or gradual extinction scenarios. The case for a catastrophic interpretation is much

stronger if many thriving taxa disappear synchronously (mass extinction), but this excludes much of the fossil record of extinction (Raup, 1994), which could therefore plausibly be driven by gradual processes instead.

Long-term evolution in the vicinity of a fitness attractor is a form of Red Queen evolution in which fitness gains are continually thwarted by environmental deterioration, resulting in effectively stagnant mean absolute fitness (Van Valen, 1973). As a consequence, persistent populations will have exponentially distributed times to extinction t_e , because extinction risk will be essentially independent of population age (ignoring short-term fitness fluctuations). However, if fitness is initially low, say because young populations tend to be colonizers in unfamiliar environments, then the risk of early extinction will be elevated (Fig. 4), and older populations will be less extinction-prone than younger ones. Intriguingly, fossil genera do exhibit reduced extinction risk with age, even after controlling for geographic range and species richness (Finnegan et al., 2008). Our results raise the possibility that population-level evolutionary processes contribute to this pattern (even without major differences in mutation rate or population size), provided that the predicted initial elevation of extinction risk lasts long enough to leave a fossil signature.

It is interesting to consider the role of genetic load in our model, since different interpretations of load have featured prominently in previous discussions about adaptation rates and extinction risk. In particular, substitutional load arguments directly contributed to the formulation and popularity of neutral theory (Kimura et al., 1968), but their interpretation was controversial. Kimura argued that most substitutions must be neutral because a many-locus version of Haldane’s single-locus substitution implies extremely large substitutional loads. However, calculating a cost of selection in this way presumes that the perfect genotype (i.e. with the fittest allele at all loci considered) is present in the population (Ewens, 2004, pp. 78). This effectively conflates the relative substitutional load (proportional to the fitness of the fittest genotype present minus mean fitness; Crow 1968) with absolute lag load (proportional to the fitness of the perfect genotype minus mean fitness; Maynard Smith 1976). In our model, the substitutional load is $q_j s$, a crucial determinant of the rate of adaptation v_j , while the lag load is $\bar{i} s$, a measure of extinction risk. The two are interdependent. In steady state this follows immediately from Eq. (4): for given population parameters, the steady state values of q_j depend on j (and therefore mean fitness \bar{i}). Or, looking at it another way, the fitness advantage of new mutants $q_j s$ determines v_j , which in turn determines the location of the fitness attractor (and if one exists).

Interdependence between these relative (substitutional) and absolute (lag) loads is a natural consequence of evolution on an absolute fitness axis driven by relative fitness differences. Substitutional and lag load can therefore be seen as complementary — but not independent — aspects of a population’s long-term evolutionary status.

Our model is superficially similar to models of mutation load accumulation (Lynch et al., 1993; Kondrashov, 1995), where, instead of environmental change, deleterious mutations gradually erode fitness. However, the effects of accumulating deleterious mutations throughout the population is potentially considerably more complicated, and much weaker, than the population-wide fitness deterioration induced by environmental shifts. For the large asexual populations considered here, provided that the deleterious mutation rate U_d is not very large ($U_d/s \ll 1$), deleterious mutations have little effect on the overall rate of fitness gain regardless of their fitness effect (Desai and Fisher, 2007). If U_d is large enough, a reversible Muller’s “ratchet” will begin to turn, shifting the entire population one fitness class at time, much like environmental change. However, either U_d would need to be very large or N very small for this mutation-induced deterioration to overpower beneficial mutant establishment and pose an extinction risk (Jiang et al., 2011; Goyal et al., 2012).

Some of the results presented here were anticipated by Bürger and Lynch (1995), particularly the pattern shown in Fig. 3b. A major focus of their analysis is what determines the critical rate of environmental change consistent with persistence ($1/T = \max_j v_j$ in our model). Their modeling assumptions are quite different from ours: sex is obligate with free recombination, and population size is small (at most 512 individuals) and effectively constant (except for after the population crosses the extinction threshold). Consequently, their population has very little linkage disequilibrium, and N is so small that genetic drift and demographic stochasticity are important factors. Our population has high linkage disequilibrium, and N is large enough that stochasticity only plays a role in the establishment of new beneficial mutations. Our approaches can therefore be viewed as complementary, but given the drastic difference in population sizes, it is hard to compare any of their specific predictions to ours.

Probably the biggest limitation of our model is that there is no genetic recombination. Sexual recombination is nearly universal among fossil species and the macroorganisms of interest to conservation biologists. This makes no difference for small populations, which are in the successional regime regard-

less of recombination. But for large populations, recombination substantially increases the rate of adaptation v_j (Neher et al., 2010; Weissman and Barton, 2012). For relatively simple models of recombination, this increase is fairly well understood (Neher et al., 2010; Weissman and Barton, 2012; Neher et al., 2013). Changing v_j does not alter the basic qualitative features of our model, particularly the central role of the fitness attractor, but would affect the quantitative predictions of persistence for given population parameters.

We have assumed that evolution slows down as the population approaches perfection because the availability of beneficial mutations is limited, represented by the fitness-dependent mutation rate Uj (running out of mutations (RM)). An alternative mechanism for slowing evolution is that beneficial mutations are less effective on fitter genetic backgrounds (diminishing returns epistasis (DR)). Since the relative importance of these alternatives is unresolved (Wiser et al., 2013; Good and Desai, 2015), we checked whether our model is sensitive to the choice of RM versus DR (Supplement C). Even for relatively strong DR, the main effect of using DR instead of RM is causing v_j to have a greater peak value which occurs at lower fitness. This does not alter our conclusions.

Acknowledgements

This work was financially supported by Wissenschaftskolleg zu Berlin and the National Science Foundation (DEB-1348262). KG is funded by NIH Grant GM084905. We thank Taylor Kessinger for early contributions to the project and Taylor Kessinger, two anonymous reviewers and the associate editor for constructive comments on the manuscript, and Mike Sanderson and Karl Flessa for helpful discussions.

References

- Laurent Augustin, Carlo Barbante, Piers RF Barnes, Jean Marc Barnola, Matthias Bigler, Emiliano Castellano, Olivier Cattani, Jerome Chappellaz, Dorthe Dahl-Jensen, Barbara Delmonte, et al. Eight glacial cycles from an antarctic ice core. *Nature*, 429(6992):623–628, 2004.
- Anthony D Barnosky, Nicholas Matzke, Susumu Tomiya, Guinevere OU Wogan, Brian Swartz, Tiago B Quental, Charles Marshall, Jenny L McGuire, Emily L Lindsey, Kaitlin C Maguire, et al. Has the Earth’s sixth mass extinction already arrived? *Nature*, 471(7336):51–57, 2011.
- Reinhard Bürger and Michael Lynch. Evolution and extinction in a changing environment: A quantitative-genetic analysis. *Evolution*, 49(1):151–163, 1995. ISSN 00143820, 15585646.
- JF Crow. The cost of evolution and genetic loads. *Haldane and Modern Biology, edited by K. Dronamraju. Johns Hopkins University Press, Baltimore*, pages 165–178, 1968.
- Charles Darwin. *On the Origin of Species*. Murray, London, 1859.
- Michael M. Desai and Daniel S. Fisher. Beneficial mutationselection balance and the effect of linkage on positive selection. *Genetics*, 176(3):1759–1798, 2007. doi: 10.1534/genetics.106.067678.
- Ulf Dieckmann and Régis Ferrière. *Adaptive dynamics and evolving biodiversity*. Cambridge University Press, 2004.
- Warren J Ewens. *Mathematical Population Genetics 1: Theoretical Introduction*. Springer Science & Business Media, 2004.
- Régis Ferrière and Stéphane Legendre. Eco-evolutionary feedbacks, adaptive dynamics and evolutionary rescue theory. *Philosophical Transactions of the Royal Society of London B: Biological Sciences*, 368(1610):20120081, 2012. ISSN 0962-8436. doi: 10.1098/rstb.2012.0081.
- Seth Finnegan, Jonathan L Payne, and Steve C Wang. The Red Queen revisited: reevaluating the age selectivity of Phanerozoic marine genus extinctions. *Paleobiology*, 34(03):318–341, 2008.

- Maria R Fumagalli, Matteo Osella, Philippe Thomen, Francois Heslot, and Marco Cosentino Lagomarsino. Speed of evolution in large asexual populations with diminishing returns. *Journal of theoretical biology*, 365:23–31, 2015.
- Richard Gomulkiewicz and David Houle. Demographic and genetic constraints on evolution. *The American Naturalist*, 174(6):pp. E218–E229, 2009. ISSN 00030147.
- Benjamin H. Good and Michael M. Desai. The impact of macroscopic epistasis on long-term evolutionary dynamics. *Genetics*, 199(1):177–190, 2015. ISSN 0016-6731. doi: 10.1534/genetics.114.172460.
- Sidhartha Goyal, Daniel J. Balick, Elizabeth R. Jerison, Richard A. Neher, Boris I. Shraiman, and Michael M. Desai. Dynamic mutation–selection balance as an evolutionary attractor. *Genetics*, 191(4):1309–1319, 2012. ISSN 0016-6731. doi: 10.1534/genetics.112.141291.
- J.B.S. Haldane. The cost of natural selection. *Journal of Genetics*, 55(3): 511–524, 1957. ISSN 0022-1333. doi: 10.1007/BF02984069.
- Xiaoqian Jiang, Zhao Xu, Jingjing Li, Youyi Shi, Wenwu Wu, and Shiheng Tao. The influence of deleterious mutations on adaptation in asexual populations. *PLoS ONE*, 6(11):1–8, 11 2011. doi: 10.1371/journal.pone.0027757.
- Motoo Kimura et al. Evolutionary rate at the molecular level. *Nature*, 217 (5129):624–626, 1968.
- Alexey S. Kondrashov. Contamination of the genome by very slightly deleterious mutations: why have we not died 100 times over? *Journal of Theoretical Biology*, 175(4):583 – 594, 1995. ISSN 0022-5193. doi: <http://dx.doi.org/10.1006/jtbi.1995.0167>.
- M. Lynch, R. Bürger, D. Butcher, and W. Gabriel. The mutational meltdown in asexual populations. *Journal of Heredity*, 84(5):339–344, 1993.
- Norman MacLeod. The geological extinction record: History, data, biases, and testing. *Geological Society of America Special Papers*, 505:1–28, 2014. doi: 10.1130/2014.2505(01).

- J. Maynard Smith. What determines the rate of evolution? *The American Naturalist*, 110(973):331–338, 1976. ISSN 00030147, 15375323.
- J. Maynard Smith. The causes of extinction. *Philosophical Transactions of the Royal Society of London B: Biological Sciences*, 325(1228):241–252, 1989. ISSN 0080-4622. doi: 10.1098/rstb.1989.0086.
- R. A. Neher, B. I. Shraiman, and D. S. Fisher. Rate of adaptation in large sexual populations. *Genetics*, 184(2):467–481, 2010. doi: 10.1534/genetics.109.109009.
- Richard A Neher, Taylor A Kessinger, and Boris I Shraiman. Coalescence and genetic diversity in sexual populations under selection. *Proceedings of the National Academy of Sciences*, 110(39):15836–15841, 2013.
- H Allen Orr. The genetic theory of adaptation: a brief history. *Nature Reviews Genetics*, 6(2):119–127, 2005.
- Eric N. Powell, John M. Klinck, and Eileen E. Hofmann. Generation time and the stability of sex-determining alleles in oyster populations as deduced using a gene-based population dynamics model. *Journal of Theoretical Biology*, 271(1):27 – 43, 2011. ISSN 0022-5193. doi: <http://dx.doi.org/10.1016/j.jtbi.2010.11.006>.
- D M Raup. The role of extinction in evolution. *Proceedings of the National Academy of Sciences*, 91(15):6758–6763, 1994.
- Steven M Stanley. Population size, extinction, and speciation: the fission effect in neogene bivalvia. *Paleobiology*, pages 89–110, 1986.
- Hildegard Uecker and Joachim Hermisson. On the fixation process of a beneficial mutation in a variable environment. *Genetics*, 188(4):915–930, 2011.
- Leigh Van Valen. A new evolutionary law. *Evolutionary theory*, 1:1–30, 1973.
- Daniel B. Weissman and Nicholas H. Barton. Limits to the rate of adaptive substitution in sexual populations. *PLoS Genet*, 8(6):1–18, 06 2012. doi: 10.1371/journal.pgen.1002740.
- Michael J Wiser, Noah Ribeck, and Richard E Lenski. Long-term dynamics of adaptation in asexual populations. *Science*, 342(6164):1364–1367, 2013.

Appendices

A: Stochastic mutant establishment

Here we summarize how the establishment probability p_{j-1} for a new mutant in fitness class $j - 1$ is calculated.

The mutant lineage's abundance is modeled with a continuous-time birth-death process with time-dependent per-capita birth $\lambda(t) = b(1 - N(t)/\kappa)$ and death $\mu(t) = d + (j(t) - 1)s$ rates, where the time dependence of j indicates that the initial fitness class of the mutant is $j - 1$, but will change to j if the environment deteriorates. This yields (Uecker and Hermisson, 2011, Eq. 16)

$$p_{j-1} = 2 \left[1 + \int_{t_m}^{\infty} (\lambda + \mu) e^{-\int_{t_m}^t (\lambda - \mu) dt'} dt \right]^{-1}, \quad (\text{A1})$$

where t_m is when the mutant is born.

Environmental change increases the mortality rate of each fitness class by s . Since the population will almost always be in demographic equilibrium before an environmental change (births \approx deaths; see Appendix C), each fitness class's death rate will exceed its birth rate by s immediately after an environmental change. In particular, the mutant's fitness advantage will be reduced by s in Eq. (A1), but will be rapidly restored to $q_j s$ as N falls to its new carrying capacity and births balance deaths again. The numerical implementation of Eq. (A1) in this case is discussed in Supplement A.

For mutants which are undisturbed by environmental change while attempting to establish, we have births \approx deaths (Appendix C), and $\lambda - \mu \approx q_j s$. Eq. (A1) can then be evaluated analytically, yielding $p_{j-1} \approx q_j s / (d + j s)$. This is the establishment probability used for our MC approximations.

B: Markov chain approximation

First, we discuss the MC approximation for the successional regime. The number of adaptive mutant establishments k_a which occur over the time required for fixation of a newly established mutant t_f (see Appendix B) when the population is in fitness class j is Poisson distributed with mean $t_f v_j$, where v_j is given by Eq. (3) and $t_f v_j \ll 1$ (Eq. (C1)). Thus, $\text{Prob}[k_a = 0] \approx 1 - t_f v_j$, $\text{Prob}[k_a = 1] \approx t_f v_j$ and $\text{Prob}[k_a > 1] \approx 0$. Similarly, $t_f \ll T$ (we are not interested in the case where T is much smaller than $1/v_j$, which implies catastrophically fast environmental deterioration), and

the probabilities that k_e mutants establish in t_f generations are $\text{Prob}[k_e = 0] \approx 1 - t_f/T$, $\text{Prob}[k_e = 1] \approx v_j/T$ and $\text{Prob}[k_e > 1] \approx 0$.

The above probabilities for k_a and k_e can be used to define the transition probabilities in an MC with iteration time of t_f and states $0 \leq j \leq i_e$. For simplicity, we instead use an MC with an iteration time of one generation, and transition probabilities

$$\begin{aligned} P(j \rightarrow j+1) &= \text{Prob}[k_e = 1]\text{Prob}[k_a = 0] = 1/T \\ P(j \rightarrow j-1) &= \text{Prob}[k_e = 0]\text{Prob}[k_e = 1] = v_j \\ P(j \rightarrow j) &= 1 - 1/T - v_j, \end{aligned} \tag{B1}$$

which behaves essentially identically because fixation takes more than one generation (there are simply more iterations between transitions).

The MC for memoryless adaptation in the multiple mutations regime can be derived in the same way, where the fixation time t_f is replaced by the time required to restore the steady-state distribution following mutant establishment at the nose. Again, this iteration time can be replaced by a single generation iteration time, yielding Eq. (B1) as before, except that v_j is given by Eq. (4) instead of Eq. (3).

In the MC for periodic adaptation in the multiple mutations regime, the iteration time is the mean establishment time $1/v_j$. One adaptive establishment occurs each iteration. The overall transition probabilities are then obtained from a Poisson distribution for the number of environmental change occurrences k_e per iteration, which has rate parameter $1/v_j T$. Thus, $P(j \rightarrow j-1) = \text{Prob}[k_e = 0]$, $P(j \rightarrow j) = \text{Prob}[k_e = 1]$, and so on.

For the memoryless MC approximations (in both the successional and multiple mutations regimes), the mean number of iterations $\langle t_e(j) \rangle$ to get from state j to the absorbing extinction state $j = i_e$ can be obtained by iterating the chain once to obtain a system of linear equations

$$\langle t_e(j) \rangle = \sum_{i=j-1}^{j+1} P(j \rightarrow i) \langle t_e(i) \rangle + 1, \quad t_e(i_e) = 0. \tag{B2}$$

For the periodic-adaptation MC, each iteration represents a state-dependent time increment $1/v_j$, and Eq. (B2) becomes

$$\langle t_e(j) \rangle = \sum_{i=j-1}^{i_{ext}} P(j \rightarrow i) \langle t_e(i) \rangle + 1/v_j, \quad t_e(i_e) = 0. \tag{B3}$$

Equations (B2) and (B3) can be solved numerically using standard built in routines e.g. `numpy.linalg.solve` in Python (analytical solution is straightforward, but the resulting solution is cumbersome Ewens 2004, Eq. 2.161).

C: Adaptation in the multiple mutations regime

Here we derive the population's steady-state rate of adaptation v_j and width q_j in the multiple mutations regime. We also introduce the concept of demographic equilibrium, a prerequisite for this derivation.

The multiple mutations regime is contrasted with the successional regime, which is characterized by such long intervals between mutation establishments that the most fit established class j will fix (reach frequency ≈ 1) well before the next mutation establishes. Suppose that the population is in equilibrium in fitness class $j + 1$ when a new mutant lineage establishes in fitness class j . Then the new mutant will initially grow exponentially at rate s , with starting population size $1/p_j$. The time t_f required for the new mutant to fix then satisfies $e^{st_f}/p_j \approx K_j$, so that $t_f \approx \ln(K_j s)/s$. For successional behavior, t_f must be much smaller than the time required for the next beneficial mutant to appear, which can be approximated by $1/v_j$ using Eq. (3) (this is a conservative lower bound assuming that the growing mutant lineage already has its fixation abundance K_j). Thus, the successional regime occurs when (Desai and Fisher, 2007)

$$t_f \approx \ln(K_j s)/s \ll 1/v_j. \quad (\text{C1})$$

The multiple mutations regime occurs when mutant lineages establish so frequently (due to high mutation rate or large N) that Eq. (C1) is violated. The successional equilibrium $N \approx K_j$ is then never realized, but the population will usually be in a state of approximate demographic equilibrium $N \approx \bar{K}$, where $\bar{K} = \sum_i K_i n_i / N$ is the time-dependent population average of the fitness-class-specific carrying capacities K_i (henceforth, overlines will denote population averages). This demographic equilibrium holds because N changes much faster than \bar{K} . With the exception of environmental change events, \bar{K} changes at a rate of

$$\frac{d\bar{K}}{dt} = -\frac{s\kappa}{b} \frac{d\bar{i}}{dt}, \quad (\text{C2})$$

where \bar{i} obeys Fisher's theorem $d\bar{i}/dt = -s(\bar{i} - \bar{i})^2$ (this version of Fisher's theorem is easily derived from Eq. (1); see Kimura et al. 1968, pp. 10).

Thus, $d\bar{K}/\kappa dt$ is typically of order s^2 between environmental disturbances. By comparison, immediately following an environmental change, N returns to the new value of \bar{K} at exponential rate s ($dN/Ndt = -s$ at the moment after the change), much faster the change in \bar{K} of order s^2 . Consequently, the per-capita birth rate is approximately $b(1 - \bar{K}/\kappa)$ (except in short intervals following environmental change). In the remainder of this Appendix, we assume that this demographic equilibrium holds.

In the multiple mutations regime, mutant establishment follows an inhomogeneous Poisson process driven by mutations in the fittest established class j . Over the time interval required for the next mutant to establish, the growth in fitness class j is approximately exponential with rate $(q_j - 1)s$ (after the next establishment this growth rate will start to decline appreciably — see below) and expected starting abundance $1/p_j$ (Eq. (2)). Thus, the expected number of mutant lineages that will have established after time t is $Ujb(1 - \bar{K}/\kappa)p_{j-1} \int_0^t e^{(q_j-1)st'} / p_j dt' \approx Ujb(1 - \bar{K}/\kappa) \int_0^t e^{(q_j-1)st'} dt'$ (the approximation uses the fact that $p_{j-1} \approx q_js/(d + js)$; see Appendix A). Setting this expected number equal 1, we can solve for the typical time t required for a newly established nose to produce the next mutant lineage that establishes, denoted t_{est} . This gives $t_{est} = \ln[(q_j - 1)s/Ujb(1 - \bar{K}/\kappa) + 1]/(q_j - 1)s \approx \ln[s/Uj]/(q - 1)s$ where $O(1)$ terms inside the logarithm have been ignored (it will become clear below that q_j is $\sim O(1)$). Thus, t_{est} only depends weakly on j over the scale of the population's fitness variation q_j (from Eq. (4), q_j is $\sim O(1)$ for the parameter regime considered here), but varies significantly over the entire fitness domain ($i_e \approx (b - d)/s$ is typically $\sim O(10)$ or $\sim O(10^2)$).

Any given fitness class keeps growing after its initial establishment until it is the most abundant fitness class, with abundance of order \bar{K} . During this process, the mean fitness \bar{i} advances, and the fitness class's fitness advantage — and growth rate — declines. In steady state, this decline in fitness advantage can be approximated as a sequence of discrete decreases of magnitude s occurring once every t_{est} generations (Desai and Fisher, 2007). Thus, the most recently established mutant, which has a mean initial abundance of $1/p_j$, grows at rate $(q_j - 1)s$ for t_{est} generations, then $(q_j - 2)s$ for another t_{est} generations, and so on, until it has abundance \bar{K} and no fitness advantage. Thus, $\bar{K} \approx \exp((q_j - 1)st_{est} + (q_j - 2)st_{est} + \dots)/p_j$. This implies that the mean fitness advances at a rate of approximately $s^2 q_j (q_j - 1)/2 \ln(K_j s)$ (again neglecting $O(1)$ terms in the logarithm). In steady state, this must match the rate of advance of the nose s/t_{est} ; setting them equals gives Eq.

(4).

Supplement

A: Numerical implementation of full simulation

Here we summarize how the full traveling wave model, illustrated in Fig. 1, is implemented numerically.

Eq. (1) is a system of coupled, nonlinear ODEs describing the dynamics of the bulk of the population. For numerical efficiency, we solve this system over the set of roughly $2q \ll i_e$ non-empty abundance classes ($n_i < 1$ is regarded as empty), where the set of non-empty classes changes over time and must be updated dynamically. We start by solving Eq. (1) for these classes from $t = 0$ up to the first environmental change at $t = T_1$, where T_1 is sampled from an exponential distribution with mean T .

Using the resulting solution, we determine the time t_m until the next mutant is produced by the fittest established class j . These births follow an inhomogeneous Poisson process with dynamic rate parameter $Ujb(1 - N(t)/\kappa)n_j(t)$. To sample t_m , we sample a normalized waiting time τ from an exponential distribution with rate parameter equal to unity, and then find the equivalent waiting time until the next mutation (in generations) for the inhomogeneous Poisson process by solving

$$\tau = \int_0^{t_m} Ujb(1 - N/\kappa)n_j dt \quad (\text{C3})$$

for t_m .

If t_m is smaller than T_1 , we check whether the variant will establish, which occurs with probability p_{j-1} (Appendix A). The numerical evaluation of Eq. (A1) is computationally expensive, so we use the following approximation scheme:

1. If the mutant does not arise near an environmental change event, demographic equilibrium implies $p_{j-1} \approx qs/(d + js)$.
2. If an environmental change occurred shortly before t_m , the mutant lineage's fitness advantage is reduced by s (Appendix A). We check for this scenario as follows. The lineage's fitness advantage takes $s/[d(\lambda - \mu)/dt|_{t=t_m}]$ generations to change by s . The disturbance from a recent environmental change is important if this timescale is comparable to or shorter than the decay timescale $\sim 1/qs$ of the integral in Eq. (A1). We then evaluate Eq. (A1) analytically assuming constant- N as for the

case of demographic equilibrium, except that N is averaged over the interval $(t_m, t_m + qs)$.

3. If the next environmental change is going to occur soon after t_m , the value of p_i is sensitive to the timing of the change and must be evaluated numerically. To do this, we solve equation Eq. (1) in an interval after T_1 .

The relative error of the resulting approximation for p_i rarely exceeds 10%.

If it is determined that the lineage does establish, at time t_m we remove any fitness classes with abundance < 1 and add the new fitness class with initial population size ν sampled from Eq. (2). We then repeat the above, starting with solving Eq. (1) over the interval from t_m to T_1 .

If t_m exceeded T_1 , we remove any fitness classes with $n_i < 1$ at T_1 and repeat the above starting with solving equation Eq. (1) over the interval from T_1 to the next sampled environmental change time T_2 .

The algorithm terminates if all fitness classes are removed; t_e is defined as the time when $N = 1$.

B: Duration of observable progression to extinction

Here we analyze the population's behavior in the period immediately preceding extinction using our MC approximation. This analysis supplements the simulation results shown in Fig. 5.

We run our MC backwards starting at time t_e , conditional on extinction occurring at t_e . The reverse time process is constructed as follows. Let Y_0, Y_1, \dots, Y_{t_e} denote the sequence of random variables describing repeated iteration of the reverse-time process i.e. $Y_\tau = X_{t_e-\tau}$ where X_0, X_1, \dots, X_{t_e} are the random variables for repeated forward-time iteration up to time t_e and τ measures time before t_e . Then, in the absence of conditions on when extinction occurs, the standard expression for backward-time transition probabilities holds:

$$\hat{P}_\tau(i \rightarrow j) = \text{Prob}[Y_{\tau+1} = j | Y_\tau = i] = \frac{p_j(t_e - \tau - 1)}{p_i(t_e - \tau)} P(j \rightarrow i), \quad (\text{S1})$$

where $p_i(t) = \text{Prob}[X_t = i]$ and P denotes forward-time transition probabilities (Appendix B).

To ensure that extinction occurs at time t_e , all three terms in Eq. (S1) must be made conditional on t_e . For $i, j \neq i_e$, $p_i(t_e - \tau)$ becomes

$$\text{Prob}[X_{t_e-\tau} = i | t_e] = \frac{\text{Prob}[t_e | X_{t_e-\tau} = i]}{\text{Prob}[t_e]} p_i(t_e - \tau), \quad (\text{S2})$$

and similarly for $p_j(t_e - \tau - 1)$, whereas $P(j \rightarrow i)$ becomes

$$\begin{aligned} & \text{Prob}[(X_{t_e-\tau} = i | X_{t_e-\tau-1} = j) | t_e] \\ &= \frac{\text{Prob}[t_e | X_{t_e-\tau} = i]}{\text{Prob}[t_e]} P(j \rightarrow i). \end{aligned} \quad (\text{S3})$$

Thus, the conditional reverse time transition matrix for $i, j \neq i_e$ is

$$\hat{P}_\tau(i \rightarrow j | t_e) = \frac{\text{Prob}[t_e | X_{t_e-\tau-1} = j]}{\text{Prob}[t_e]} \hat{P}_\tau(i \rightarrow j) \quad (\text{S4})$$

For our problem of reconstructing the pre-extinction behavior of populations which persist for long times, the reverse time transitions Eq. (S4) are independent of τ to an excellent approximation. Long-term persistence implies that in the period preceding extinction, the forward-time process has

had enough time to reach quasi-equilibrium (i.e. the probability of finding the chain in a given state conditional on non-extinction is independent of the initial state — the initial state has been “forgotten”). Then $\hat{P}_\tau(i \rightarrow j)$ becomes

$$\hat{P}(i \rightarrow j) = \frac{p_j(t_e - \tau - 1)}{p_i(t_e - \tau)} P(j \rightarrow i) = c \frac{m_j}{m_i} P(j \rightarrow i) \quad (\text{S5})$$

where m_j is the quasi-stationary probability of being in state j (i.e. $m_j = \lim_{t \rightarrow \infty} m_j(t)$ where $m_j(t) = \text{Prob}[X_t = j | \text{not extinct}]$), and $c = 1/(1 - \sum_{i \neq i_e} m_i P(i \rightarrow i_e))$ is a normalization constant. The quasi-stationary distribution m_j can be obtained by repeated iteration of the forward-time process using the fact that $m_j(t) = p_j(t)/(1 - p_{i_e}(t))$.

The term $\text{Prob}[t_e | X_{t_e - \tau - 1} = j] / \text{Prob}[t_e]$ in Eq. (S4) is more troublesome. It must equal 1 if τ is sufficiently large and j is sufficiently distant from i_e , since then the condition $X_{t_e - \tau - 1} = j$ has no bearing on the risk of extinction at the distant time τ in the future. To gain some insight into when this breaks down, we can rewrite the term as

$$\frac{f(\tau, j)}{\sum_i f(\tau, i) m_i} \quad (\text{S6})$$

where $f(\tau, k) = \text{Prob}[t_e, X_{t_e - \tau - 1} = k | \text{not extinct}]$. In other words, the ratio deviates from 1 when $f(\tau, j)$ deviates from its expectation with respect to the quasi-stationary distribution. The greatest potential deviations occur at j values near the extinction threshold i_e where m_j is essentially zero i.e. precisely those states incompatible with long-term persistence. Specifically, if $f(\tau, j)$ is localized at these values, say because τ is so small that extinction is imminent, the deviation from 1 may be quite large. But clearly this only applies to τ values that are tiny compared to the duration of the fluctuating traversal process from the fitness attractor to i_e . For essentially all values of τ , the deviation can never be so large as to counteract its multiplication by the corresponding near-zero values of m_j in Eq. (S4). Accordingly, this term can be set to 1 to an excellent approximation.

Fig. 5 shows the expected behavior of the fittest established class j immediately preceding extinction using the reverse-time transition matrix $\hat{P}(i \rightarrow j)$ to calculate the reverse-time state probability distribution $p_j(t_e - \tau | \text{not extinct})$ (we use the memoryless adaptation approximation for $P(j \rightarrow i)$ to avoid the complication of variable size iteration times). For comparison

between MC and simulations, we shift the simulation expectation horizontally so that for both the MC and simulations, $\tau = 0$ when $i = i_e$. This accounts for the time it takes for the population to die off after crossing the extinction threshold i_e in the simulations, which is not accounted for in the MC approximation.

C: Running out of mutations vs. diminishing returns epistatis

Here we show that a variant of our MC approximation (Appendix B) which uses a diminishing returns (DR) instead of a running out of mutations (RM) mutation model produces similar long-term behavior.

To model DR, we replace the fixed fitness increment s with geometric increments $s_i \propto R^{-i}$ ($0 < R < 1$) (Fumagalli et al., 2015), where s_i is the fitness increment between classes i and $i+1$, and the mortality rate in fitness class i is $d + \sum_{k=0}^{i-1} s_k$. Smaller R represents stronger diminishing returns.

With the change from s to s_i , it is no longer possible to keep the fitness effect of environmental deterioration independent of i as it is for RM. Environmental change shifts the population backwards by some integer amount, say $k(i)$, and in general the resulting change in fitness ($s_i + s_{i+1} + \dots + s_{i+k(i)-1}$) will not be the same for all i no matter how $k(i)$ is chosen. We determine $k(i)$ numerically by minimizing the difference between the resulting fitness change and a “goal” environmental change fitness effect s/T .

The DR mutation rate U^* is independent of fitness. For comparison with RM, U^* is set equal to the RM beneficial mutation rate Uj averaged over the RM quasistationary distribution m_j (see text after Eq. (S5) in Supplement B).

Fig. S1 compares RM and DR mean extinction times as a function of T , making the appropriate changes to Eq. (4) for the DR case. DR extinction times tend to be larger (for given s/T), because $s_i > s$ when i is closer to extinction than perfection. This has multiple effects, increasing the establishment probability, the size of each fitness jump, and the strength of selection in the bulk of the population. This has a powerful combined effect at low fitness, which outweighs the linear (successional), or sub-linear (multiple mutations) low-fitness benefit of greater mutational availability Uj .

When diminishing returns is weak ($R = 0.97$), RM and DR are very similar (Fig. S2). Fixing T for RM, and bringing the RM and DR fitness attractors into approximate agreement by reducing T in the DR model ($T = 151$ compared with $T = 180$ for RM), the net rate of fitness increase is similar over most of the fitness domain, and the quasistationary distributions almost coincide. Thus, the difference between these models is primarily a rescaling of the adaptation rate v_j .

For stronger diminishing returns ($R = 0.94$), the discrepancy is more substantial (Fig. S3). Apart from the fact that a larger change in T is

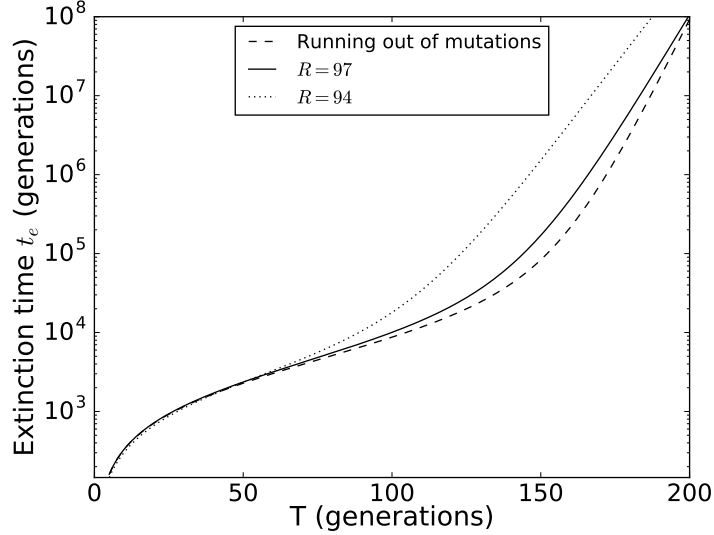


Fig. S1: Mean extinction times for weak DR ($R = 0.97$) are similar to those for RM. Stronger DR ($R = 0.94$) causes a more substantial discrepancy. Same parameters as Fig. 3.

required to bring the fitness attractors together ($T = 125$ compared with $T = 180$ for RM), the shape of v_j is significantly different over the entire fitness domain, with DR v_j several times larger than RM v_j near extinction. The quasistationary distributions have similar shapes, although in the DR case this corresponds to far fewer fitness classes — a dense cluster of classes at high fitness is essentially unreachable. This has the effect of “smoothing” the transition to persistence (Fig. S1) in much the same way that increasing s in the RM model does: the fitness attractor becomes less and less relevant the fewer states there are in its vicinity to act as a basin of attraction. However, this also implies that long-term evolution is driven exclusively by large effect mutations, which is probably not realistic. Correcting for this by appropriately increasing i_e for the DR model would again restore the basic qualitative structure of our long-term extinction model, particularly the central role of the fitness attractor. Thus, even fairly strong DR does not substantially alter our predictions.

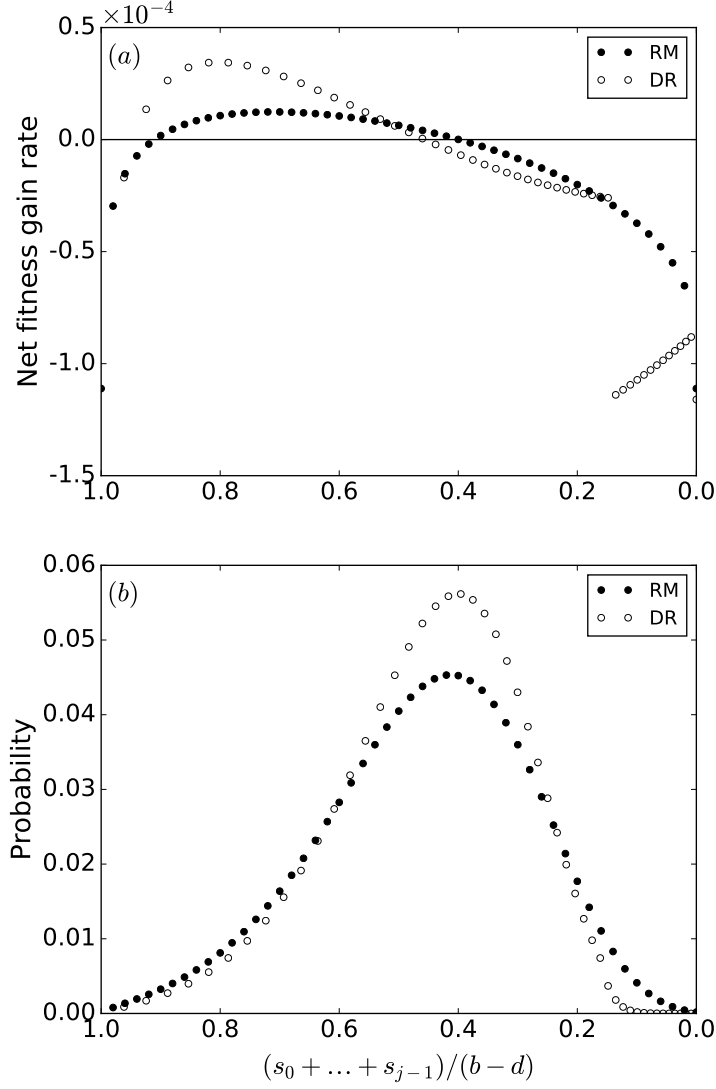


Fig. S2: For weak DR ($R = 0.97$), RM and DR models behave similarly aside from greater DR v_j . For comparison, we offset the higher DR v_j by adjusting T (DR $T = 151$, DM $T = 180$). (a) Net rate of fitness increase (i.e. v_j minus environmental deterioration rate) is similar except at high fitness. DR is discontinuous due to the fitting procedure for environmental deterioration fitness jumps. (b) With the v_j offset, quasistationary distributions are essentially the same. Same parameters as Fig. S1 (apart from T offset).

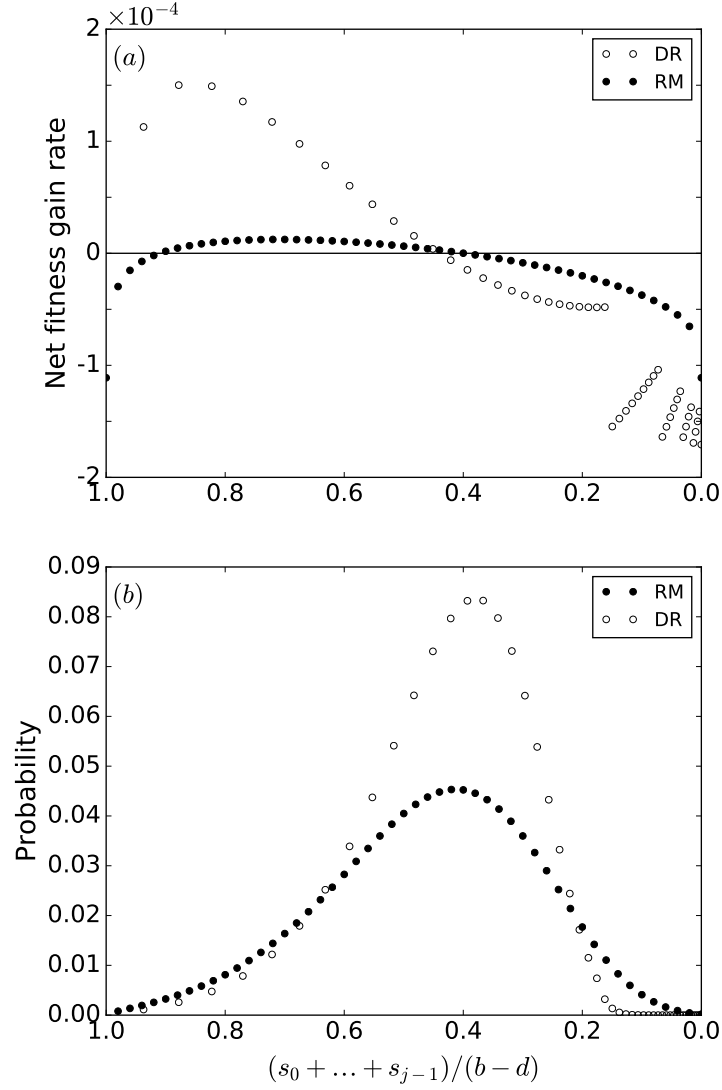


Fig. S3: Same as Fig. S2 but with stronger diminishing returns ($R = 0.94$). Now RM and DR models differ more substantially. As in Fig. S2, we offset v_j by adjusting T (DR $T = 125$, DM $T = 180$). Otherwise same parameters as Fig. S2.